J. Hydrol. Hydromech., 65, 2017, 1, 26–34
DOI: 10.1515/johh-2016-0048

Study of the time-dependent clear water scour around circular bridge piers

Aysegul Ozgenc Aksoy[1*], Gokcen Bombar[2], Tanıl Arkis[1], Mehmet Sukru Guney[1]

[1] Civil Engineering Department, Dokuz Eylul University, Tinaztepe Campus, Izmir, Turkey.
[2] Civil Engineering Department, Ege University, Bornova, Izmir, Turkey.
[*] Corresponding author. Tel.: 00902323017054. E-mail: aysegul.ozgenc@deu.edu.tr

Abstract: The local scour around bridge piers influences their stabilities and plays a key role in the bridge failures. The estimation of the maximum possible scour depth around bridge piers is an important step in the design of the bridge pier foundations. In this study, the temporal evolution of local scour depths as well as the equilibrium scour depths were analyzed.

The experiments were carried out in a rectangular flume by using uniform sediment with median diameter of 3.5 mm and geometric standard deviation of 1.4. The diameters of the tested circular bridge piers were 40 mm, 80 mm, 150 mm and 200 mm. The flow and scour depths were determined by ultrasonic sensors. The experiments were realized in clear water conditions with various constant flow rates.

The experimental findings were compared with those calculated from some empirical equations existing in the literature. A new empirical relation involving the flow intensity, the relative water depth and the dimensionless time is also introduced. The advantage of this proposed relation is that the only parameter requiring the calculation is the critical velocity, other parameters being known geometric and hydraulic parameters. The performance of this relation was tested by using experimental data available in the literature, and a satisfactory compatibility was revealed between the experimental and numerical results.

Keywords: Bridge pier; Clear-water scour; Local scour; Steady flow; Temporal evolution.

INTRODUCTION

Up to now, many clear water scour experiments were carried out and numerous empirical equations were derived to estimate the equilibrium scour depth, e.g., Hancu (1971), Breusers et al. (1977), Melville and Sutherland (1988), Melville (1997), Richardson and Davis (2001), and Sheppard et al. (2004). The temporal evolution of the scour depth is also an important issue to understand the scour process. Most of the existing studies are focused on the equilibrium scour depth values and the experiments about the temporal variation of the scour depths are rather scarce. Yanmaz and Altinbilek (1991) studied the time-dependent scour depth in steady flow conditions by using uniform bed material and a semi-empirical time-dependent analysis of local scour depths around bridge piers has been conducted using the sediment continuity equation for the scour hole around bridge piers. Kothyari et al. (1992) proposed a method considering the primary vortex in front of the pier to compute the temporal variation of the scour depth. Melville and Chiew (1999) investigated the influence of the flow duration on the local scour depth around cylindrical bridge piers in uniform sand beds. They proposed a method to determine the time for the development of the equilibrium scour depth and the concomitant estimation of the scour depth at any stage during development of the equilibrium scour hole. Oliveto and Hager (2002) studied the temporal evolution of the scour depth around bridge piers and abutments in clear water conditions, by measuring sediment surface with the so-called shoe gauge having a horizontal base of 4 mm by 2 mm. They proposed an equation for the temporal scour evolution and verified it with available literature data. Later, they extended their scour formula to spur dikes and studied the effect of unsteady flow (Oliveto and Hager, 2005). Mia and Nago (2003) proposed a method to predict the time dependent local scour depth. They indicated that the equilibrium local scour depth is reached when the bed-shear stress tends to the critical value in the scour hole. Chang et al. (2004) performed experiments with uniform and non-uniform sediments and they investigated the sediment size variation of surface bed materials around the pier nose. Kothyari et al (2007) proposed a new relationship for the temporal scour evolution by relating the scour depth to the difference between the actual and the entrainment densimetric particle Froude numbers.

Guney et al. (2013) used Ultrasonic Velocity Profiler (UVP) in order to record the time varied bed elevations, by recognizing that the peak of the echo amplitudes corresponds to the bottom surface.

Although many factors causing scour around bridge piers and abutments are known, the researches in this area couldn't go further away from suggestions of a new empirical equation due to the complexity of the scour process. Each researcher investigated the process by considering some of the effective factors under certain assumptions.

The main objective of this study is to investigate the temporal variation of the scour depth around circular bridge pier by performing elaborate measurements and to suggest an empirical equation as accurate as possible.

THEORETICAL BACKGROUND

The parameters effecting the local scour around a bridge pier are the flow parameters such as mean flow velocity (V), approach flow depth (y), fluid density and viscosity (ρ and μ), bed material (sediment) characteristics (median size d_{50}, geometric standard deviation σ_g, sediment density ρ_s, critical velocity V_c), pier geometry (pier width L, pier shape and alignment) and time (time t, time to reach the equilibrium scour depth t_e, duration of the flow t_d).

The local scour depth can be expressed as a function of flow intensity (V/V_c), relative approach flow depth (flow shallowness, y/L), relative sediment size (sediment coarseness, d_{50}/L) and time by assuming constant relative density of sediment and

neglecting the viscous effects on sediment transport (Melville and Chiew, 1999).

The critical velocity V_c was determined from the logarithmic velocity profile distribution (Melville and Sutherland, 1988):

$$\frac{V_c}{u_{*c}} = 5.75 \log\left(5.53 \frac{y}{d_{50}}\right) \quad (1)$$

where u_{*c} denotes the critical shear velocity, and it was found by using the second of the following relations based on the Shields diagram (Melville, 1997):

$$u_{*c} = 0.0115 + 0.0125 d_{50}^{1.4} \quad \text{if } 0.1 \text{ mm} < d_{50} < 1 \text{ mm} \quad (2)$$

$$u_{*c} = 0.0305 d_{50}^{0.5} - 0.0065 d_{50}^{-1} \quad \text{if } 1 \text{ mm} < d_{50} < 100 \text{ m} \quad (3)$$

In these relations is in m/s and the sediment size d_{50} is in mm.

The time to reach the equilibrium scour depth was generally increased with the pier diameter. Simarro et al. (2011) indicated that the equilibrium scour depth cannot be specified for experiments shorter than one to two weeks. However, the equilibrium scour depths calculated below were generally found close to the measured final scour depths. Therefore, the duration of the experiment (t_d) is taken into consideration rather than the time to reach the equilibrium scour depth (t_e).

The temporal evolutions of the dimensionless scour depth (d_s/D) versus dimensionless time (t/t_d) are presented in Figure 3. The final values of dimensionless scour depth were found decreasing with diameter and increasing with discharge.

The equilibrium scour depths were determined by using the following mathematical functions given in Sheppard et al. (2004):

$$d_s(t) = \mathrm{a}\left[1 - \frac{1}{(1+abt)}\right] + \mathrm{c}\left[1 - \frac{1}{(1+cdt)}\right] \quad (4)$$

and

$$d_s(t) = a\left[1 - \exp(-bt)\right] + c\left[1 - \exp(-dt)\right] \quad (5)$$

where $d_s(t)$ is the scour depth at time t and a, b, c, d are coefficients to be found by the conventional least squares method.

Some of the relations predicting the time dependent local scour depth are as follows:

Melville and Chiew (1999) suggested the following relation:

$$d_s = K_{yD}\ K_I\ K_d\ K_t \quad (6)$$

where K_{yD} is the flow depth-pier width expression (m), K_I is the flow intensity factor, K_d is the particle size factor and K_t is the time factor.

Oliveto and Hager (2002) proposed Eq. (7) to predict the temporal local scour depth variation.

$$Z = 0.068\ N \sigma^{-1/2} F_d^{3/2} \log(T) \quad (7)$$

where Z is the dimensionless scour depth ($Z = z(t)/L_R$; $z(t)$ is the scour depth, L_R is the reference length), N is the shape coefficient and taken 1 for the circular pier, and σ is the standard deviation ($= (d_{84}/d_{16})^{1/2}$). F_d is the densimetric Froude particle number ($F_d = V/\left(g' d_{50}\right)^{1/2}$ where $g' = \left[\left(\rho_s - \rho\right)/\rho\right] g$ and T is the dimensionless time which is expressed as $T = \left[\left(g' d_{50}\right)^{1/2} / L_R\right] t$).

Kothyari et al. (2007) proposed:

$$Z = 0.272\ \sigma^{-1/2} \left(F_d - F_{d\beta}\right)^{2/3} \log(T) \quad (8)$$

where $F_{d\beta}$ is the densimetric particle Froude number for the inception of the scour.

EXPERIMENTAL RESEARCH

The experimental studies were carried out in a rectangular flume 0.80 m wide and 18.6 m long. The transparent side walls of the flume made from plexiglas were 0.75 m high. The slope of the flume was fixed to 0.006. The pump was connected to the speed control unit capable to control the flow rate by adjusting the settings. The discharges were measured by the electromagnetic flow meter OPTIFLUX 1000 (manufactured by Krohne with measurement range of –140 l/s ~ +140 l/s). The ULS– 40D (manufactured by General Acoustics with measurement range of 30 mm~3.4 m, resolution up to 0.18 mm, repetition rate up to 75 Hz) level monitoring system was used for water level measurements. The velocity profiler UVP (manufactured by MetFlowSA) was used to measure temporal scour depth values. The transducers with 4 MHz frequency were used in this study.

The sketch of the experimental set-up and the positions of the sensors are given in Figure 1. The bed was fixed with small concrete blocks at the first 3 m part of the flume. The total length of the mobile bed was 15.6 m. The thickness of the approximately uniform sediment layer was 0.26 m. Before each experiment, the flume bed was leveled by a mobile system moving on the rails over the side walls along the flume. Circular bridge piers having a diameter D of 40 mm, 80 mm, 150 mm and 200 mm were used. The tested bridge piers were placed at 11.5 m from the upstream end of the channel.

The bed material used in the flume was uniform with d_5 = 1.81 mm, d_{16} = 2.26 mm, d_{50} = 3.47 mm, d_{84} = 4.41 mm, and d_{95} = 4.90 mm, determined by the sieve analysis. Its geometric standard deviation (σ_g) was 1.39. The bed material was quartz sand with specific weight of 2.65 t/m^3 and the particles were manufactured in rounded shape.

The experiments were carried out by using four different steady discharges; Q of 52 l/s, 56 l/s, 61 l/s and 66 l/s. At the beginning of the experiments the discharge was gradually increased to the desired value by means of a regulation valve while the tail gate at the downstream of the flume was kept closed. The tail gate was then opened gradually in order not to disturb the bed material. The details of the experiments are given in Table 1 at which Fr is Froude number ($Fr = V/(g.y)^{(1/2)}$) and d_s denotes final scour depth. The final scour depth was measured at three different locations, namely the upstream, downstream and left side of the pier. The duration of each experiment was selected as 400 minutes, because beyond this value the rate of change of the scour depth was negligibly small.

The temporal variations of the scour depth at upstream face of the piers are given in Figure 2 for different discharges.

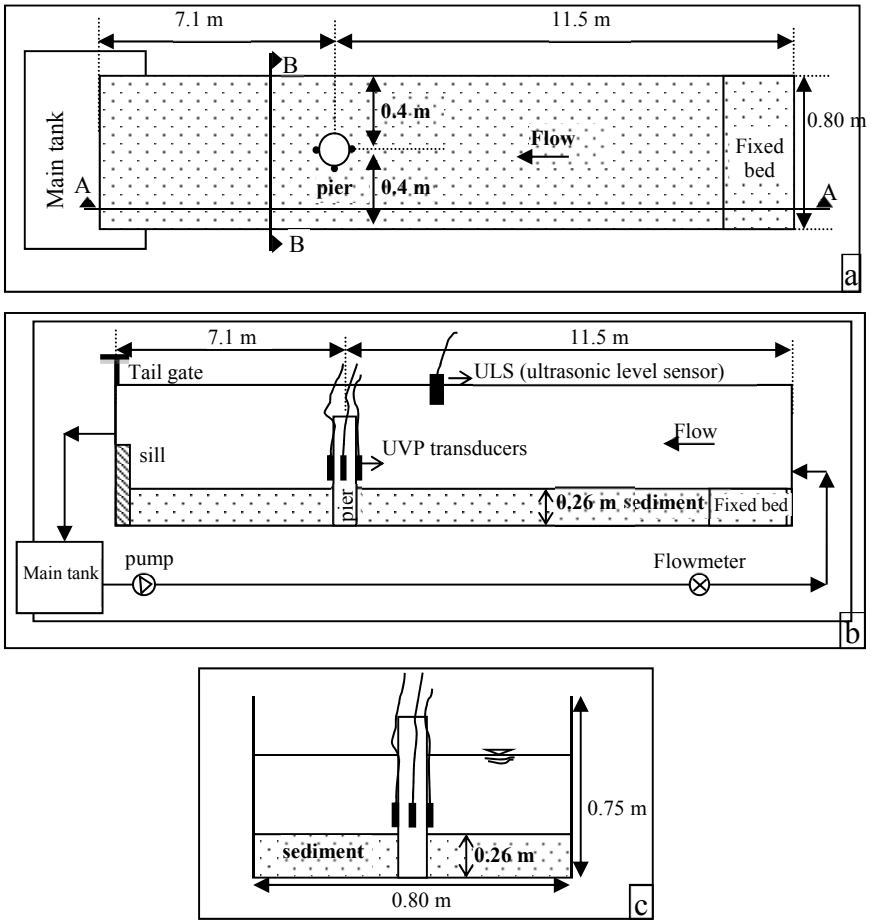

Fig. 1. Scheme of the experimental set-up a) Plan view b) Longitudinal section (A-A section) c) Cross section (B-B section).

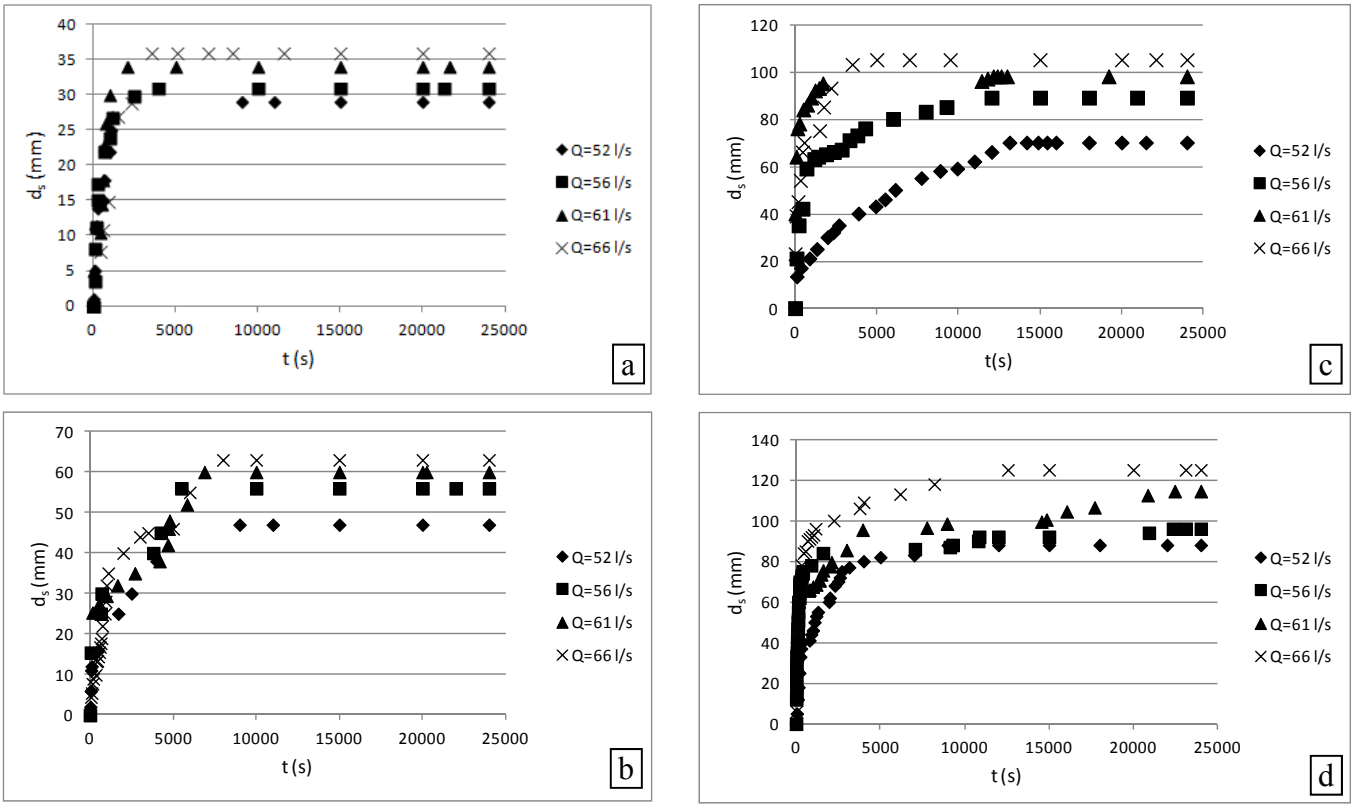

Fig. 2. Temporal evolutions of the scour depth for the pier of diameter a) 40 mm, b) 80 mm, c) 150 mm, d) 200 mm, for different flow rates.

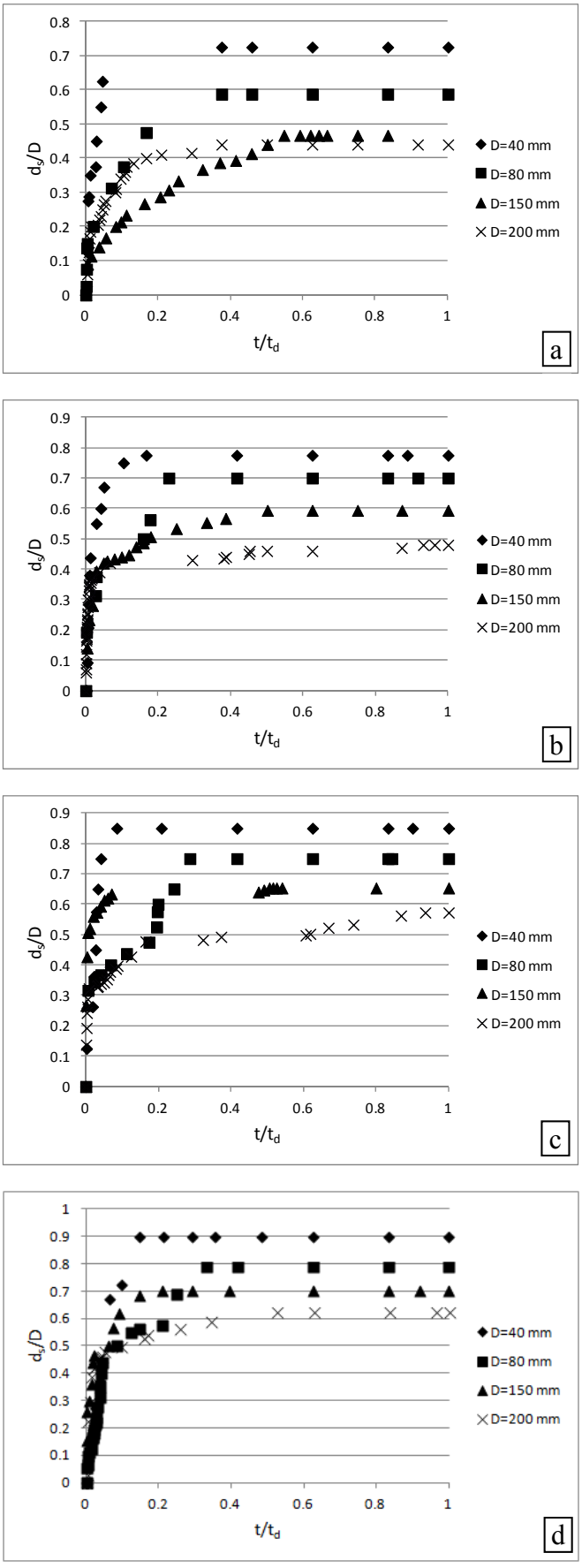

Fig. 3. Evolutions of dimensionless scour depth values versus dimensionless time for a) Q = 52 l/s, b) Q = 56 l/s, c) Q = 61 l/s, d) Q = 66 l/s.

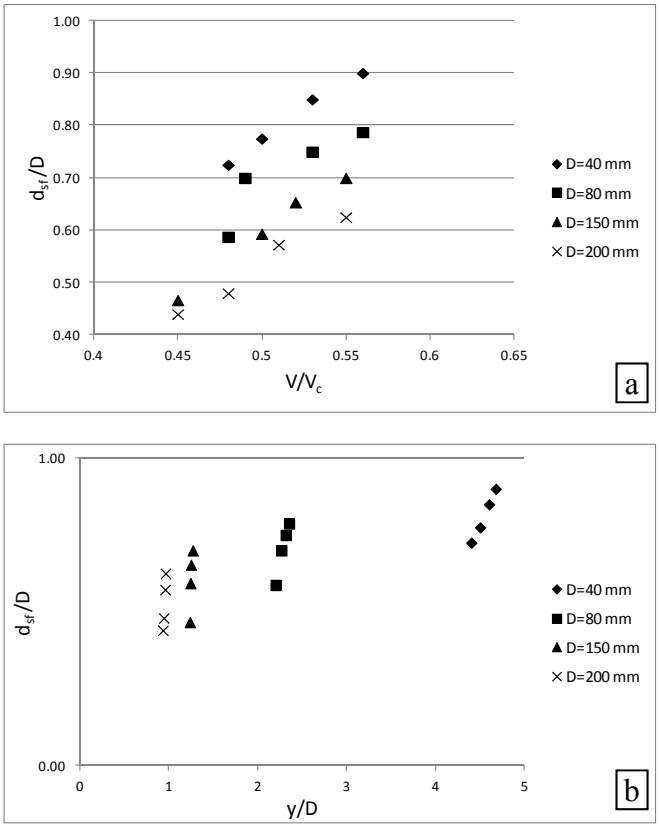

Fig. 4. Variations of the dimensionless final scour depth versus a) flow intensity b) dimensionless approach flow depth.

Table 1. Details of the experiments and measured final scour depths.

Experiment name	D (mm)	Q (l/s)	Y (mm)	V/V_c	Fr	d_s (mm)
S-4-1	40	52	176	0.48	0.28	29
S-4-2	40	56	180	0.50	0.29	31
S-4-3	40	61	184	0.53	0.31	34
S-4-4	40	66	187	0.56	0.33	36
S-8-1	80	52	176	0.48	0.28	47
S-8-2	80	56	181	0.49	0.29	56
S-8-3	80	61	185	0.53	0.31	60
S-8-4	80	66	188	0.56	0.32	63
S-15-1	150	52	185	0.45	0.26	70
S-15-2	150	56	186	0.50	0.29	89
S-15-3	150	61	187	0.52	0.30	98
S-15-4	150	66	190	0.55	0.32	105
S-20-1	200	52	186	0.45	0.26	88
S-20-2	200	56	188	0.48	0.27	96
S-20-3	200	61	191	0.51	0.29	114.5
S-20-4	200	66	192	0.55	0.31	125

DISCUSSION OF RESULTS AND COMPARISONS

During the experiments, the maximum scour depths were first observed at the pier side and then migrated to the upstream face of the pier.

The greater the pier diameter and the higher the flow velocity, the greater scour depth was observed, as expected.

The experimental results revealed that the dimensionless scour depths increased with the flow intensity. The influence of the dimensionless approach flow depth (y/D) was more perceptible when the pier diameter was greater.

Table 2. Calculated equilibrium scour depths and depths measured at the end of the each experiment.

Experiment Name	$d_{se\_Eq.4}$ (mm)	$d_{se\_Eq.5}$ (mm)	$d_{se\_measured}$ (mm)
S-4-1	29.8	28.9	29
S-4-2	32.4	30.5	31
S-4-3	36.1	34.4	34
S-4-4	40.4	36.5	36
S-8-1	50.2	47.4	47
S-8-2	57.5	56.4	56
S-8-3	61.9	62.0	60
S-8-4	69.2	61.4	63
S-15-1	83.9	74.3	70
S-15-2	86.9	86.4	89
S-15-3	95.7	94.8	98
S-15-4	105.4	105.2	105
S-20-1	91.3	87.1	88
S-20-2	91.9	97.1	96
S-20-3	127	109.5	114.5
S-20-4	119.9	115.9	125

Once the coefficients in Eqs. (4) or (5) were determined, the equilibrium scour depth was obtained by substituting $t = \infty$. The so calculated equilibrium scour depths and those measured at the end of the each experiment, that is, the final scour depths are given in Table 2. The measured final scour depths were found nearly at the same order of magnitude with the calculated equilibrium scour depths, and they were closer to those obtained from Eq. (5).

The variations of the dimensionless final scour depth (d_{sf}/D) versus flow intensity and dimensionless approach flow depth are given in Figure 4a and 4b, respectively.

A new empirical relation, the most compatible with our experimental results, was investigated by using the dimensionless time parameter proposed by Yanmaz and Altinbilek (1991). The proposed relation was obtained by using the least squares method which minimizes the sum of squared residuals. The so obtained Eq. (9) is as follows:

$$\frac{d_s}{D} = 0.8\left(\frac{V}{V_c}\right)^{\frac{3}{2}}\left(\frac{y}{D}\right)^{0.15}\left(\log T_s\right)^{0.6} \tag{9}$$

at which T_s is the dimensionless time parameter which can be expressed as follows (Yanmaz and Altinbilek, 1991):

$$T_s = t\, d_{50}\left(\Delta\, g\, d_{50}\right)^{0.5} / D^2 \tag{9a}$$

where $\Delta = \left(\rho_s - \rho\right)/\rho$.

The advantage of this empirical equation is that the only parameter requiring the calculation is the critical velocity since other parameters are the known geometric and hydraulic parameters. This feature makes this relation much more convenient for practical uses.

The comparison between the experimental results and those computed from various empirical relations are given in Figure 5. The results obtained from the proposed relation (Eq. 9) show a good accord with the experimental findings. The agreement for the scour depth values computed from Eq. (7) was fairly good for large pier diameters (D = 150 mm and D = 200 mm) compared to smaller diameters (D = 40 mm and D = 80 mm). According to the numerical results obtained from Eq. (8) the scour was not occurred at all around the pier having the diameter of 40 mm, and the scour around the pier with the diameter of 80 mm were underestimated. The scour depths computed by using Eq. (6) were overestimated in all cases.

Table 3. Geometric and hydraulic parameters of previous studies.

Experiment No (*)	D (mm)	y (cm)	d_{50} (mm)	t_d (min)	V/V_c
1	67	16.5	1.07	360	0.89
2	67	15.2	1.07	330	0.86
3	67	13.5	1.07	360	0.88
18	57	10.5	1.07	300	0.75
23	47	10.5	1.07	240	0.75
25	47	16.5	1.07	360	0.93
A1	60	16.0	1.28	300	0.71
A2	60	20.0	1.28	140	0.75
A3	60	23.5	1.28	270	0.78
A4	60	27.0	1.28	210	0.80
A5	60	30.0	1.28	270	0.82
S1	100	2.0	1.00	1140	1.38
S2	100	2.0	1.00	1140	0.99
S5	100	3.0	0.71	420	1.35
S6	100	1.5	0.71	420	0.82
Shp-1	110	119	0.22	5340	0.87
Shp-2	310	119	0.22	9780	0.93
Shp-3	910	127	0.80	21600	0.85
Shp-4	910	87	0.80	8580	0.87
Shp-5	310	127	0.80	5280	0.83
Shp-6	110	127	0.80	2460	0.87
Shp-7	910	122	2.90	11280	0.90
Shp-8	910	56	2.90	19800	0.84
Shp-9	910	29	2.90	26880	0.83
Shp-10	910	17	2.90	36960	0.70
Shp-11	910	190	2.90	21000	0.75
Shp-12	310	122	0.22	15360	1.21
Shp-13	310	18	0.22	12960	1.10
Shp-14	910	181	0.22	34800	0.86
E1	152	42	0.27	1740	0.63
E10	152	43	0.84	1130	0.90
E22	152	43	0.84	19920	0.61

(*) 1,2,3,18,23,25- Yanmaz & Altinbilek (1991) ; A1,A2,A3,A4,A5- Mia and Nago (2003) ; S1,S2,S5,S6- Chang et al (2004); Shp-1 to Shp-14- Sheppard et al. (2004); E1, E10, E22- Sheppard and Miller (2006)

Table 4. SSE (%) values for each equation.

Eq. 6	Eq. 7	Eq. 8	Proposed Eq. 9
35.4	9.5	21.8	5.1

Our suggested relation was tested by using the experimental findings obtained by Yanmaz and Altinbilek (1991), Mia and Nago (2003), Chang et al. (2004), Sheppard et al. (2004), and Sheppard and Miller (2006), as illustrated in Figures 6, 7, 8, 9 and 10, respectively. An acceptable compatibility was revealed between the computed results obtained from our relation and these experimental results. In Figures 6,7,8 and 9b whose original forms were duplicated from the corresponding publications, the results computed from Eq. 9 by using the data of the mentioned experiments are denoted by "COM-experiment no". The geometric and hydraulic parameters corresponding to these experiments are summarized in Table 3.

The statistical convenience of the proposed Eq. (9) was tested by applying Fisher (f) test. The f value was computed as 197.1 The critical value of f for the 0.01 significance level is 6.70. Consequently, the significance of our proposed relation (Eq. 9) is demonstrated.

The errors associated with the measured scour depths and those predicted by using the formulas mentioned above were computed for each experiment, by means of the sum of squared errors (SSE). Calculated SSE values for each equation are given in Table 4.

The SSE value being minimum for our proposed relation justifies its statistical consistency.

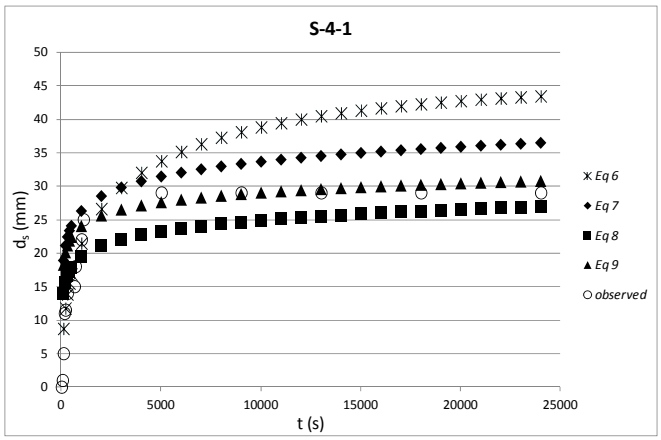

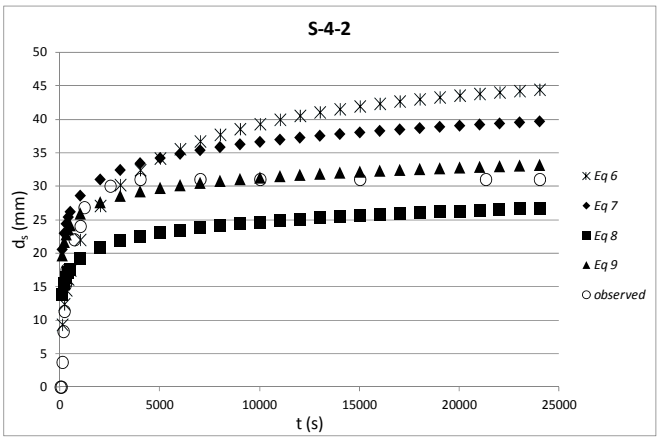

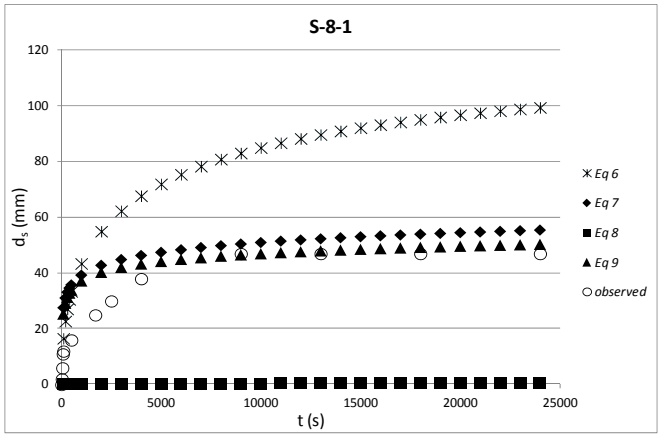

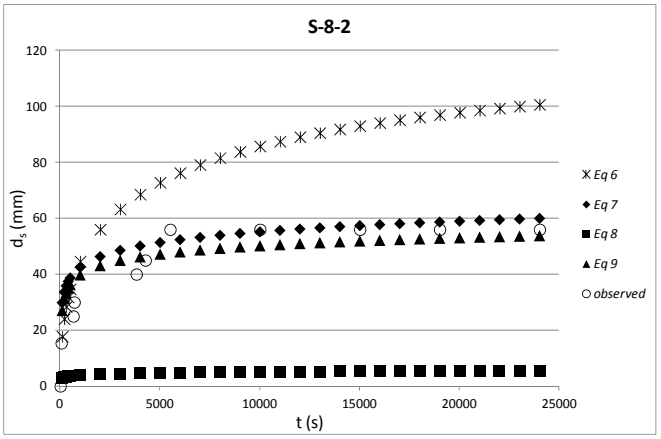

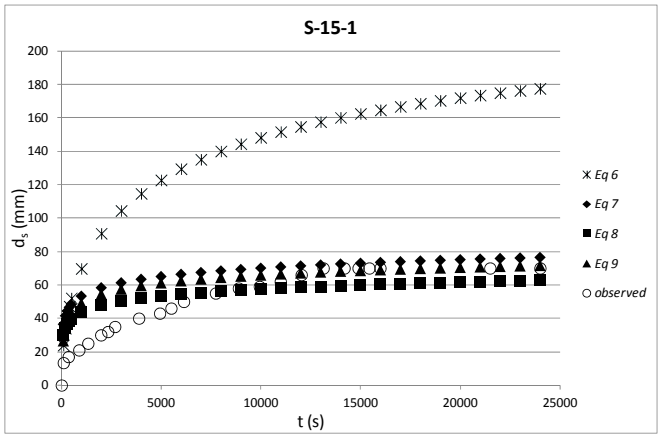

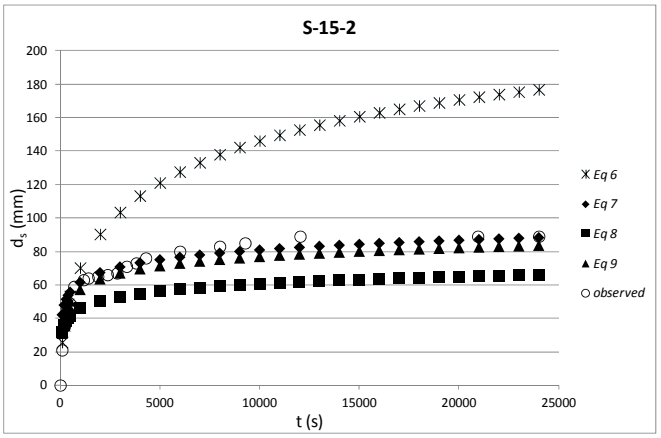

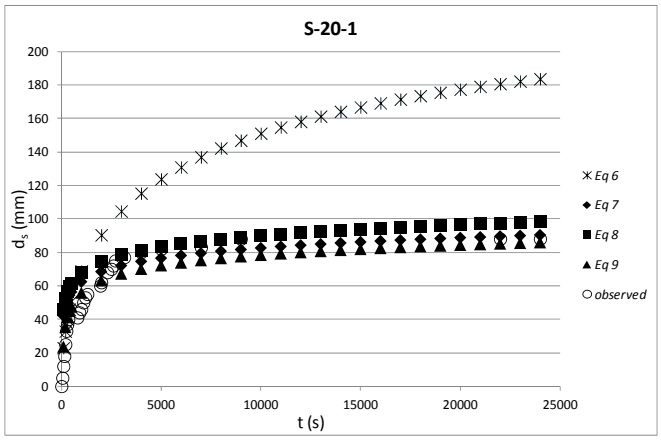

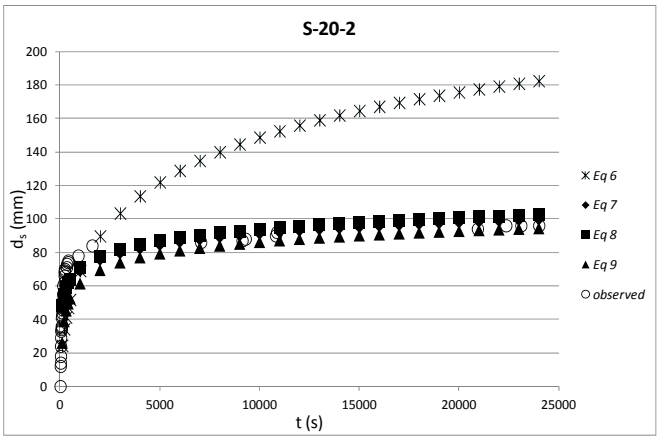

Fig. 5a. Computed and measured temporal variations of the scour depths for Q = 52 l/s.

Fig. 5b. Computed and measured temporal variations of the scour depths for Q = 56 l/s.

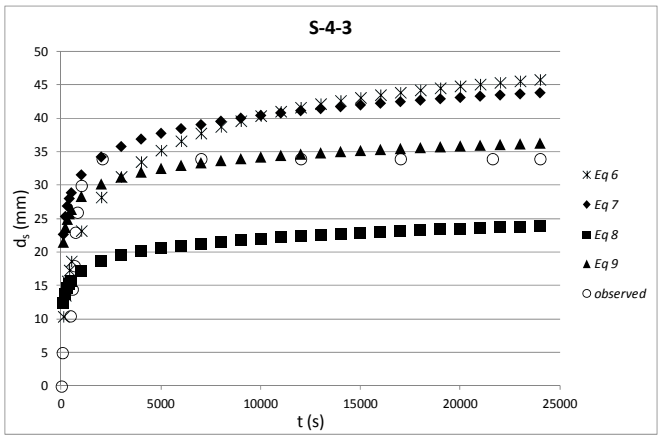

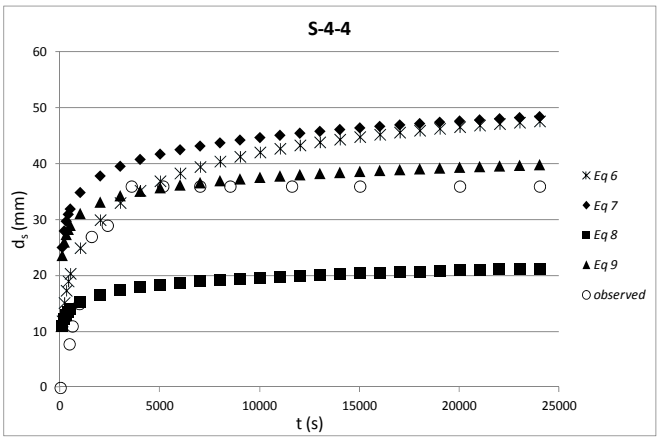

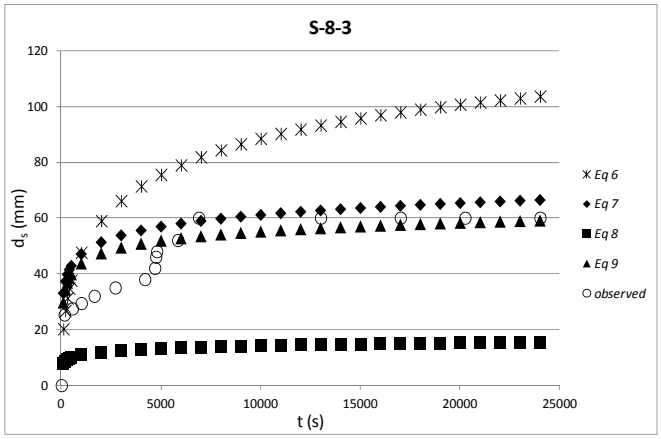

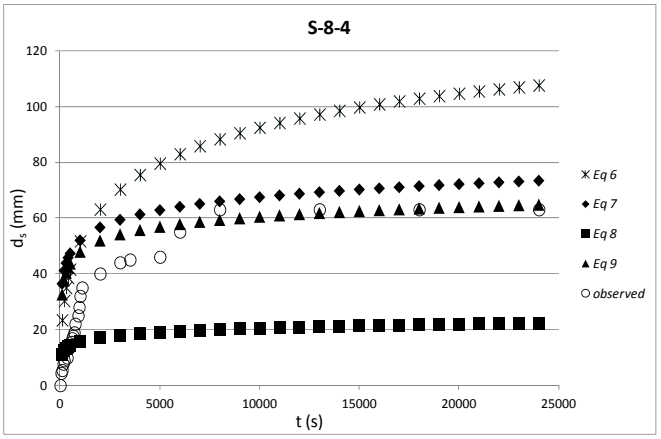

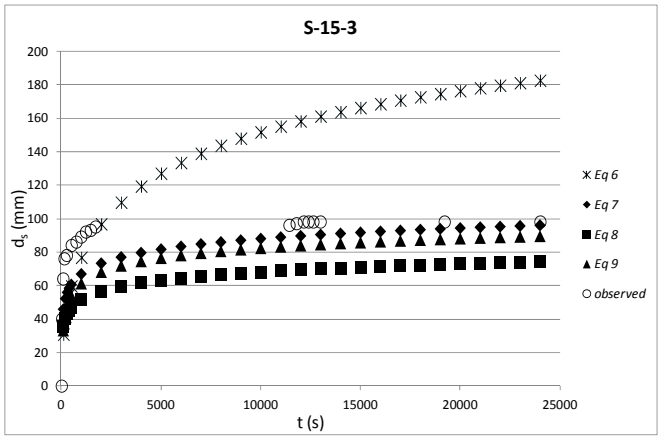

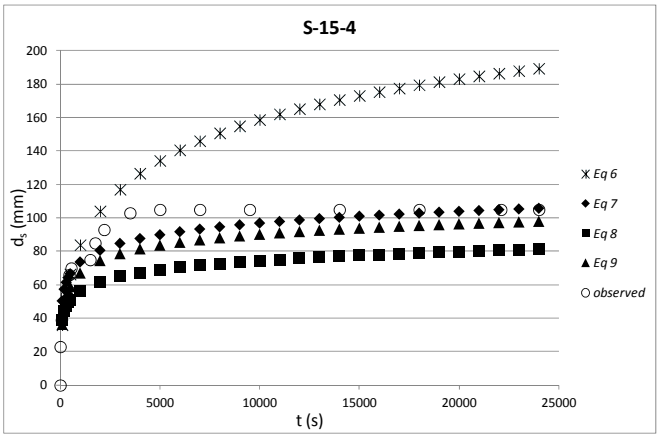

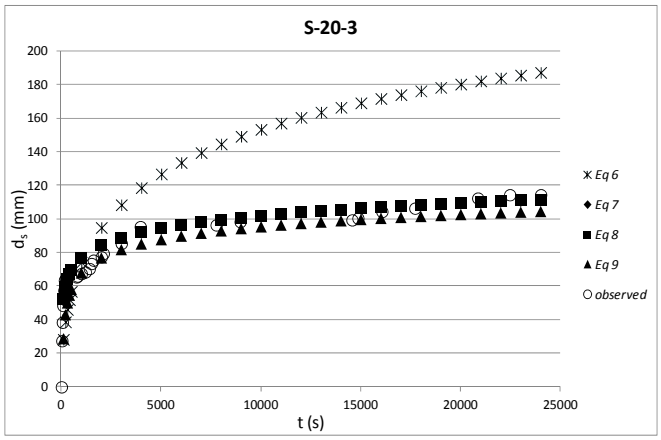

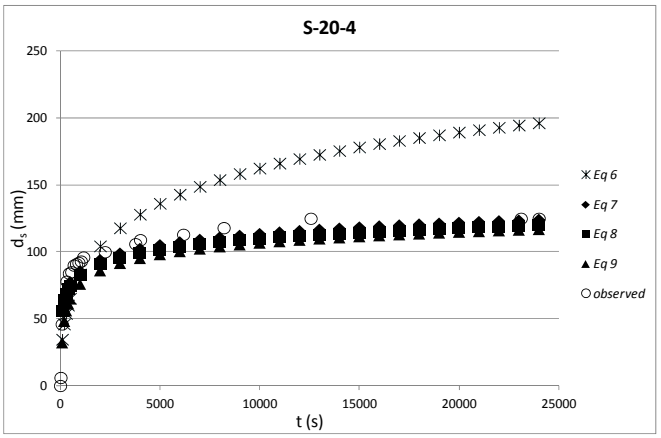

Fig. 5c. Computed and measured temporal variations of the scour depths for Q = 61 l/s.

Fig. 5d. Computed and measured temporal variations of the scour depths for Q = 66 l/s.

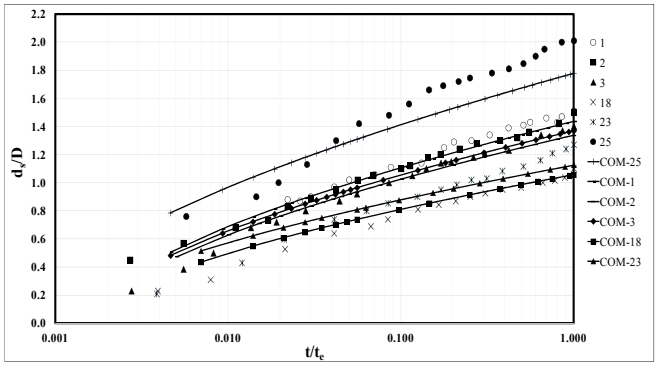

Fig. 6. Comparison of the temporal variations of the dimensionless scour depth computed from the suggested relation with those observed by Yanmaz and Altinbilek (1991).

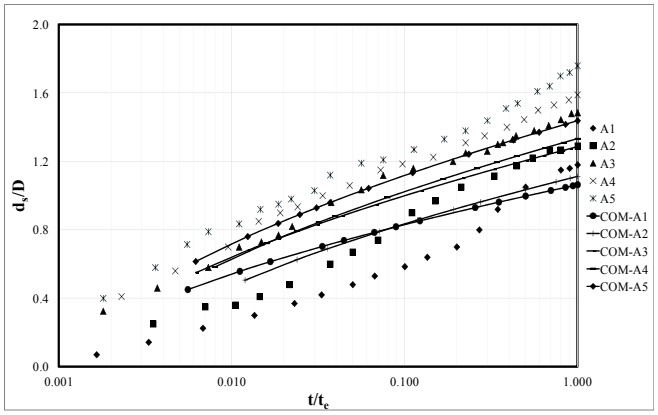

Fig. 7. Comparison of the temporal variations of the dimensionless scour depth computed from the suggested relation with those observed by Mia and Nago (2003).

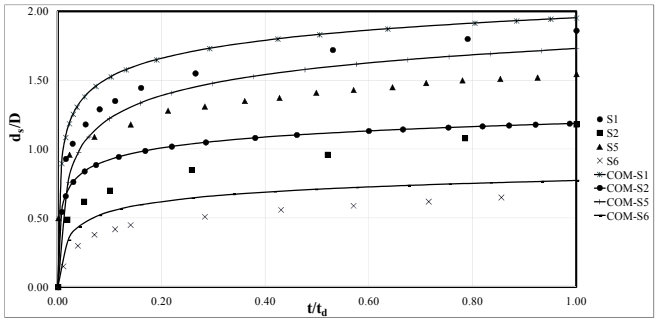

Fig. 8. Comparison of the temporal variations of the dimensionless scour depth computed from the suggested relation with those observed by Chang et al. (2004).

CONCLUSION

In this study, the temporal variation of the scour depths around circular bridge pier was investigated experimentally. The experimental results revealed that the scour depth was increased with the pier diameter and flow velocity. The time to reach the final scour depth was generally increased with the pier diameter.

A new specific relation to predict the time evolution of the scour depths was proposed by using the experimental findings. This suggested formula is fairly convenient compared to those

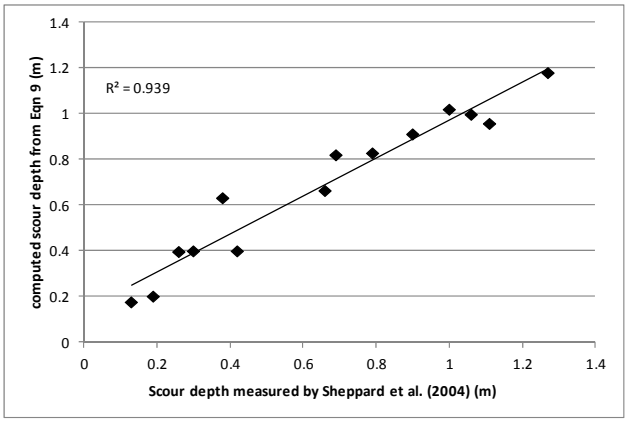

Fig. 9a. Comparison of the scour depths computed from the suggested relation and those measured by Sheppard et al. (2004).

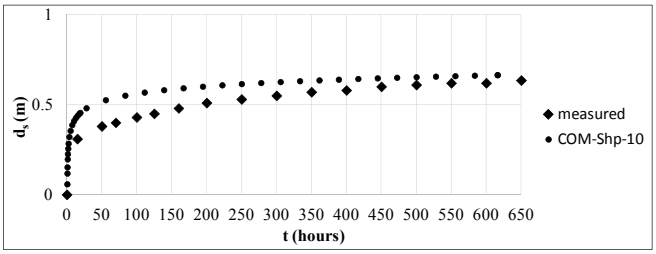

Fig. 9b. Comparison of the time dependent scour depths computed from the suggested relation and those measured by Sheppard et al. (2004).

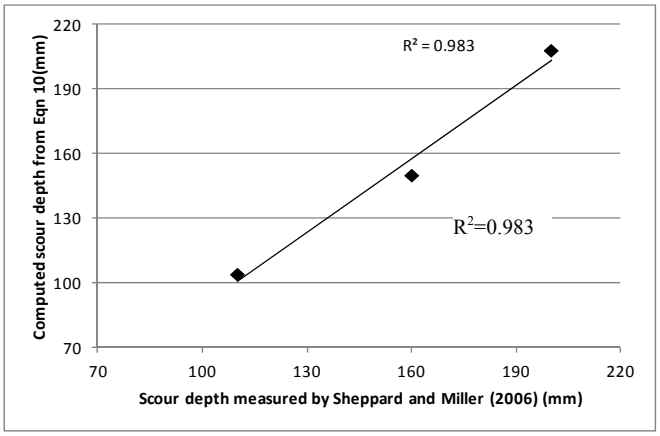

Fig. 10. Comparison of the scour depths computed from the suggested relation and those measured by Sheppard and Miller (2006).

available in the literature. The advantage of this empirical equation is that the only parameter requiring the calculation is the critical velocity since other parameters are the known geometric and hydraulic parameters. This feature makes this relation much more convenient for practical uses. This relation was also tested by using the experimental data obtained previously by some authors and an acceptable compatibility was observed between their experimental findings and the numerical results obtained from the proposed relation.

The statistical convenience of the proposed relation was tested and confirmed by applying Fisher (f) test and computing the sum of squared errors.

Acknowledgement. The authors thank TÜBİTAK (project number 106M274 and 109M637) for the financial support.

REFERENCES

Breusers, H.N.C., Nicollet, G., Shen, H.W., 1977. Local scour around cylindrical piers. Journal of Hydraulic Resources, 15, 3, 211–252.

Chang, W.Y., Lai, J.S., Yen, C.L., 2004. Evolution of scour depth at circular bridge piers. Journal of Hydraulic Engineering, 130, 9, 905–913.

Guney, M.S., Bombar, G., Aksoy, A.O., Dogan, M., 2013. Use of ultrasonic velocity profiler (UVP) to investigate the evolution of bed configuration. KSCE Journal of Civil Engineering, 17, 5, 1–10.

Hancu, S., 1971. Sur le calcul des affouillements locaux dans la zone des piles des ponts. In: Proc. 14th AHR Congr. Int. Assn. for Hydr. Res. (IAHR), Paris, France, Vol. 3, pp. 299–313.

Kothyari, U.C., Garde, R.J., Ranga Raju, K.G., 1992. Temporal variation of scour around circular bridge piers. Journal of Hydraulic Engineering, 118, 8, 1091–1106.

Kothyari, U.C., Hager, W.H., Oliveto, G., 2007. Generalized approach for clear-water scour at bridge foundation elements. Journal of Hydraulic Engineering, 133, 11, 1229–1240.

Melville, B.W., 1997. Pier and abutment scour: Integrated approach. Journal of Hydraulic Engineering, 123, 2, 125–136.

Melville, B.W., Chiew, Y.M., 1999. Time scale for local scour at bridge piers. Journal of Hydraulic Engineering, 125, 1, 59–65.

Melville, B.W., Sutherland, A.J., 1988. Design method for local scour at bridge piers. Journal of Hydraulic Engineering, 114, 10, 1210–1226.

Mia, F., Nago, H., 2003. Design method of time-dependent local scour at circular bridge pier. Journal of Hydraulic Engineering, 129, 6, 420–427.

Oliveto, G., Hager, W.H., 2002. Temporal evolution of clear-water pier and abutment scour. Journal of Hydraulic Engineering, 128, 9, 811–820.

Oliveto, G., Hager, W.H., 2005. Further results to time-dependent local scour at bridge elements. Journal of Hydraulic Engineering, 131, 2, 97–105.

Richardson, E.V., Davis, S.R., 2001. Evaluating Scour at Bridges. 4th Ed. Hydraulic Engineering Circular No. 18, Federal Highway Administration Publication No. FHWA-NHI 01-001, Washington, DC, 376 p.

Sheppard, D.M., Miller, W., 2006. Live-bed local pier scour experiments. Journal of Hydraulic Engineering, 132, 7, 635–642.

Sheppard, D.M., Odeh, M., Glasser, T., 2004. Large scale clearwater local pier scour experiments. Journal of Hydraulic Engineering. 130, 10, 957–963.

Simarro, G., Fael, C., Cardoso, A., 2011. Estimating equilibrium scour depth at cylindrical piers in experimental studies. Journal of Hydraulic Engineering, 137, 9, 1089–1093.

Yanmaz, M., Altinbilek, H.D., 1991. Study of time-dependent local scour around bridge piers. Journal of Hydraulic Engineering, 117, 10, 1247–1268.

NOMENCLATURE

D pier diameter
d_{50} median size of the bed material (sediment)
d_s scour depth
$d_s(t)$ the scour depth at time t
d_{sf} final scour depth
d_{sf}/D dimensionless final scour depth
d_{50}/D (d_{50}/L) relative sediment size
d_s/D dimensionless scour depth
Fr Froude number
F_d densimetric Froude particle number
$F_{d\beta}$ densimetric particle Froude number for the inception of the scour
g gravitational acceleration
g' $\left\{\left[\left(\rho_s-\rho\right)/\rho\right]g\right\}$ reduced gravitational acceleration
K_{yD} flow depth-pier width expression (L)
K_I flow intensity factor
K_d particle size factor
K_t time factor
L pier width
N shape coefficient
Q discharge
t time
t_e time to reach the equilibrium scour depth
t_d flow duration
t/t_d dimensionless time
T dimensionless time $\left(T=\left[\left(g'd_{50}\right)^{1/2}/\ L_R\right]t\right)$
T_s dimensionless time parameter $\left(T_s=t\,d_{50}\left(\Delta\,g\,d_{50}\right)^{0.5}/D^2\right)$
u_{*c} critical shear velocity
V mean flow velocity
V_c critical velocity
V/V_c flow intensity
y approach flow depth
y/D (y/L) relative approach flow depth
Z dimensionless scour depth
μ dynamic viscosity
ρ_s sediment density
ρ fluid density
σ_g geometric standard deviation of the sediment

Received 10 November 2015
Accepted 15 June 2016